arXiv:1401.1371v3 [astro-ph.CO] 14 Nov 2015

Circular Polarization of the CMB: A probe of the First stars

Soma De[1], Hiroyuki Tashiro[2]
[1] *School of Earth and Space Exploration, Arizona State University, Tempe, AZ 85287, USA*
[2] *Physics Department, Arizona State University, Tempe, AZ 85287, USA*

While it is revealed that the Cosmic Microwave Background (CMB) is linearly polarized at 10 % level, it is predicted that there exists no significant intrinsic source for circular polarization (CP) in the standard cosmology. However, during the propagation through a magnetised plasma, the CP of the CMB could be produced via the Faraday conversion (FC). The FC converts a pre-existing linear polarization into CP in presence of a magnetic field with relativistic electrons. In this paper, we focus on the FC due to supernova remnants of the first stars, also called Pop III stars. We derive an analytic form for the angular power spectrum of the CP of the CMB generated by the general FC. We apply this result to the case of the FC triggered by explosions of the first stars and evaluate the angular power spectrum, C_l^{VV}. We show that the amplitude of $l(l+1)C_l^{VV}/(2\pi) > 10^{-2}\mu\mathrm{K}^2$ for $l > 100$, with only one Pop III star per halo, the age of Pop III SN remnants as 10^4 years and frequency of CMB observation as 1 GHz. We expect the CP of the CMB to be a very promising probe of the yet unobserved first stars, primarily due to the expected high signal along with an unique frequency dependence.

I. INTRODUCTION

Observations of the Cosmic Microwave Background (CMB) are essential in modern cosmology. In particular, a precise measurement of the CMB polarization is one of the major goals for ongoing and future CMB observations. Theoretical studies of the CMB polarization predict a 10% level in linear polarization under standard cosmology [3–6]. The linear polarization of the CMB can be produced by anisotropic Thomson scattering around the epoch of recombination [1, 2]. Since the first detection of CMB polarization anisotropy by DASI [7], several observations have measured the angular power spectrum of the polarization and the cross-correlation with the CMB temperature anisotropies (e.g., Ref. [8] for one of recent works). These observational results are consistent with the theoretical predictions of the cosmological observables that follow from the standard ΛCDM model. On the other hand, the circular polarization (CP, hereafter) of the CMB is usually assumed to be zero, because there is no generation mechanism at the epoch of recombination within the standard cosmology.

However, the CP of the CMB can be created in the free-streaming regime *after* the epoch of recombination. One of such generation mechanism is the Faraday conversion (FC) which is formalized by the generalized Faraday rotation. Due to the FC, the linear polarization of the CMB can be converted to the CP with the presence of relativistic magnetized plasma [10, 11]. The FC could be expected when the CMB propagate through relativistic magnetized plasma in galaxy clusters. Ref. [12] has shown that the FC due to galaxy clusters might be able to create the CP at the level of 10^-9 at frequencies of 10 GHz.

The CP of the CMB can be generated by other mechanism. Mohammadi have investigated the generation of the CP of the CMB through their scattering with the cosmic neutrino background [13]. Giovannini has shown that the curvature perturbations can produce the CP with the presence of primordial magnetic fields around the last scattering surface [14, 15]. Sawyer has discussed the CP due to photon-photon interactions mediated by neutral hydrogen background [16]. In addition, some new physics effects can induce the CP of the CMB [17–19].

Recently Mainini et al. have performed the first attempt to detect the CP of the CMB since '90 [20]. They have improved the upper limit on the degree of the CP, which is between 5×10^{-4} and 0.4×10^{-4} at large angular scales (between 8° and 24°). However, this limit is very far from 10^{-9} degree of the CP predicted in a cosmological context.

In this paper, we evaluate the CP of the CMB via the FC in supernova (SN) remnants of the first stars. The formation of the first stars is a important milestone in the evolution of the structure formation. After photon decoupling, overdensity regions began to grow and collapsed to dark matter halos. Inside of dark matter halos, formation of luminous objects like stars was not solely driven by gravity and requires a sufficient amount of baryon gas cooling inside of a dark matter halo, to eventually form stars. These first born stars are thought to be very massive and are termed as the first stars or alternatively Pop III stars. It is believed that Pop III stars formed in small halos (10^6-10^8 $M_\odot$) at $z \sim$ 20-30 (see Refs. [21, 22] for recent reviews). Although Pop III stars are key to early structure formations as the first luminous objects and the sources of cosmic reionization and cosmic metal pollution, no Pop III stars have been directly observed and there is some debate on their properties including mass range of Pop III stars. In the isolation scenario, Pop III star mass is predicted to be massive, 100–500 $M_\odot$ [23–28].

It is known that Pop III stars with mass > 10 $M_\odot$ cause SNe at their death. The detection of SNe of Pop III stars are expected as one of the possible probes of first stars as these SNe could be much brighter than their progenitors or

host galaxies. In particular, Pop III stars with 140-260 $M_\odot$ could explode as pair-instability SNe, which is up to 100 times more energetic than Type Ia and Type II SNe [29]. Many works have been done to investigate the observability of Pop III SNe [30–38]. According to these works, SNe of Pop III stars could be found by the James Webb Space Telescope (JWST) or the Wide-Field Infrared Survey Telescope (WFIRST). Additionally, SN remnants of Pop III stars may be also detectable. Meiksin and Whalen have found that SN remnants of Pop III stars in 10^7 $M_\odot$ halos can produce observable radio signatures [39]. Oh et al. have shown that SN remnants of Pop III stars may induce additional CMB temperature anisotropy through the Sunyaev-Zel'dovich effect [40].

In this paper, we adopt a simple analytic model for the evolution of SN remnants to study the FC in a SN remnant of a Pop III star. Our aim is to evaluate the anisotropy of the CMB CP. We calculate the power spectrum of the FC by using the halo formalism [41], then we compute the angular power spectrum of the CMB CP. Throughout this paper, we adopt a flat ΛCDM cosmology, with $h = 0.7$, $\Omega_c = 0.23$, and $\Omega_b = 0.046$.

II. CIRCULAR POLARIZATION DUE TO FARADAY CONVERSION

Due to the Thomson scattering with the presence of quadrapole temperature anisotropy, the CMB becomes linearly polarized during the epoch of recombination. As the CMB propagates through inter-galactic medium and galaxy clusters, there are secondary effects which are imprinted on the CMB temperature anisotropy and polarization properties.

One of such secondary effects is the creation of the circular polarization (CP) in the CMB through the mechanism of Faraday Conversion (FC). The FC can be understood in the following way. Consider a linearly polarized electromagnetic (EM) wave in a homogeneous magnetized plasma. Let the direction of propagation of the EM wave be orthogonal to the direction of the external magnetic field in the plasma. This linearly polarized EM wave can be decomposed into two linear polarized waves with the same phase, perpendicular and parallel to the external magnetic field. Circular polarization of an EM wave can be visualized as two linear polarized waves with a phase difference between the linearly polarized components. Charged particles in the plasma are free to move along the magnetic field lines and can respond easily to the electric field of the EM wave. However, the motions of the charged particles perpendicular to the magnetic field lines are affected by the magnetic field and their response to the electric field of the EM wave is now modified. Therefore, a difference arises in the particle motions between the two orthogonal polarization directions of the EM field, due to the existence of the magnetic field in the plasma. This difference translates into a phase difference between two linearly polarized components of the EM wave parallel and perpendicular to the external magnetic field. As a result, a circularly polarized wave is generated.

In this section, after giving a brief review of the Stokes parameters, we formulate the generation of the CP of the CMB due to the FC to obtain the analytic form of the CP angular power spectrum.

A. Stokes parameters

First of all, we consider a monochromatic EM wave propagating along $\hat{z}$. This EM wave is characterized by two mutually perpendicular electric field components on the x-y plane. At a given point in space, the amplitude of the electric field vectors pointing along $\hat{x}$ and $\hat{y}$ respectively are described by [42]

$$\begin{aligned} E_x &= E_x^0(t)\cos(\omega t - \phi_x(t)), \\ E_y &= E_y^0(t)\cos(\omega t - \phi_y(t)). \end{aligned} \tag{1}$$

The extent of polarization is generally quantified in terms of the so-called Stokes parameters I, Q, U and V. These Stokes parameters for a monochromatic EM wave are defined as

$$\begin{aligned} I &= (E_x^0)^2 + (E_y^0)^2, \\ Q &= (E_x^0)^2 - (E_y^0)^2, \\ U &= 2E_x^0 E_y^0 \cos(\phi_x - \phi_y), \\ V &= 2E_x^0 E_y^0 \sin(\phi_x - \phi_y). \end{aligned} \tag{2}$$

However, in practice, we measure EM waves at a frequency ω with a bandwidth $\Delta\omega$. That is, measured EM waves can be expressed as a superposition of many waves around ω. For such EM waves, the Stokes parameters are obtained

by the time averaging of the electric field components of the EM waves,

$$\begin{aligned} I &= \langle (E_x^0)^2 \rangle + \langle (E_y^0)^2 \rangle, \\ Q &= \langle (E_x^0)^2 \rangle - \langle (E_y^0)^2 \rangle, \\ U &= \langle 2E_x^0 E_y^0 \cos(\phi_x - \phi_y) \rangle, \\ V &= \langle 2E_x^0 E_y^0 \sin(\phi_x - \phi_y) \rangle, \end{aligned} \tag{3}$$

where the bracket $\langle\ \rangle$ denotes the time averaging with the time interval over which the measurement is performed.

As shown in above equations, the I parameter represents the intensity of the EM waves, the Q and U parameters are associated to the LP of the EM waves and the V parameter quantifies the extent of the CP. The parameters I and V are coordinate-independent (scalar) and dimensionless true observables. The parameters Q and U transform under a rotation of the coordinate system while $Q^2 + U^2$ is an invariant under the rotation of the axes. The sign of the parameter V related to the rotating direction of electric field components on the x-y plane. EM waves with $V > 0$ and $V < 0$ are called, respectively, right-handed and left-handed circular polarized waves. A linearly polarized wave is a combination of one left circularly and one right circularly polarized waves with equal amplitudes, that is, $V = 0$. A circularly polarized wave is created when the left and right circularly polarized components have unequal amplitudes.

B. Angular power spectrum of circular polarization

For the analysis of the CMB anisotropy, it is useful to perform an angular decomposition of the anisotropic values in multipole space. Let $V(\hat{n})$ be the CP at a given direction $\hat{n}$ on the sky. Since the Stokes parameter V is a scalar quantity, it can be expanded in the basis of scalar spherical harmonics $Y_{lm}(\hat{n})$ in the following way,

$$V(\hat{n}) = \sum_{lm} V_{lm} Y_{lm}(\hat{n}). \tag{4}$$

Using the coefficients V_{lm}, we can write the angular power spectrum of the CMB circular polarization, C_l^{VV}, as

$$C_l^{VV} = \frac{1}{2l+1} \sum_m V_{lm} V_{lm}^*. \tag{5}$$

Let us consider the CP of the CMB due to the FC. The observed CP is given in terms of the Stokes V parameter by [10]

$$V(\hat{n}) = -2 \int_{r_*}^{0} dr\ U(r, \vec{x}, \hat{n}) \alpha(r, \vec{x}, \hat{n}, \hat{b}), \tag{6}$$

where r is the comoving distance, $*$ denotes the value at the last scattering surface and $U(\vec{x}, \hat{n})$ is the Stokes parameter at a comoving space position $\vec{x}$ and observation direction $\hat{n}$ with $\vec{x} = r\hat{n}$. Here $\alpha(r, \vec{x}, \hat{n}, \hat{b})$ is the FC rate with the magnetic field direction $\hat{b}$, which we will discuss in more detail in the next section. As shown in Eq. (A5) of the appendix, $\alpha(r, \vec{x}, \hat{n}, \hat{b})$ can be decomposed as

$$\alpha(r, \vec{x}, \hat{n}, \hat{b}) = 2\pi \sqrt{\frac{32\pi}{15}} \int \frac{d^3k}{(2\pi)^3} \tilde{\alpha}(z, k) \left({}_2Y_2^0(\hat{n}) + {}_{-2}Y_2^0(\hat{n}) \right) \sum_l (-i)^l j_l(kr) \sum_{m=-l}^{m=l} Y_{lm}^*(\hat{k}) Y_{lm}(\hat{n}), \tag{7}$$

where ${}_{\pm 2}Y_l^m(\hat{n})$ are spin-2 spherical harmonics, $j_l(x)$ is the spherical Bessel function, and, for simplicity, we assume that $\hat{b}$ is $(0, 0)$ in a polar coordinate system for the sky, $\hat{b} = (\theta, \phi)$.

Generally, the stokes parameters for a linear polarization, U and Q, can be expanded as [6]

$$(Q \pm iU)(r, \vec{x}, \hat{n}) = \int \frac{d^3k}{(2\pi)^3} \sum_l \sum_{m=-2}^{m=2} (E_{lm} \pm iB_{lm})_{\pm 2} G_l^m(\vec{x}, -\hat{n}), \tag{8}$$

where ${}_{\pm 2}G_l^m$ is a mode function for a spin-2 field,

$${}_{\pm 2}G_l^m(\vec{x}, \hat{n}) = (-i)^l \sqrt{\frac{4\pi}{2l+1}}\ {}_{\pm 2}Y_l^m(\hat{n}) e^{i\vec{k}.\vec{x}}. \tag{9}$$

In Eq. (8), E_{lm} and B_{lm} are coefficients for so-called E- and B-mode polarizations [3–6]. For simplicity, we assume that B-mode polarization vanishes hereafter. In this assumption, the parameter U is given in terms of E_{lm} as

$$2iU(r,\vec{x},\hat{n}) = \int \frac{d^3k}{(2\pi)^3} \sum_l \sum_{m=-2}^{m=2} E_{lm} \left({}_2G_l^m - {}_{-2}G_l^m\right). \tag{10}$$

With Eqs. (7) and(10), we can decompose the Stokes parameter $V(\hat{n})$ in Eq. (6) in spherical harmonics as shown in Eq. (4). After a lengthy calculation, we finally obtain the angular power spectrum of V as

$$C_l^{VV} \approx \frac{128}{15\pi} \sum_{l'l''l'''} \sum_{m'=-2}^{m'=2} \sum_{m''+m'''=m} \int_{r_*}^{0} dr \int \frac{k^2dk}{(2l'+1)r^2} P_\alpha\left(r, \frac{l''}{r}\right) P_{E_{lm}}(r,k)\, j_{l'''}^2(kr) I_{lm}^2, \tag{11}$$

where $P_{E_{lm}}(r,k)$ is the power spectrum of the E-mode polarization, E_{lm}, at a comoving distance r, $P_\alpha(r,k)$ is the power spectrum of the FC rate at r, and I_{lm} is given by Eq. (A12). Note that the detailed derivation of Eq.(11) is in the appendix and P_α has a dimension of (length). Eq. (11) conveys that, depending on the power spectrum, $P_\alpha(r,k)$, the E-mode polarization is converted to the CP.

It is worth discussing the implications carried by Eq. (6). This equation quantifies a transfer of polarization from an existing Stokes U into V, via the FC mechanism. As we will see in the following section, α in Eq. (6) depends only on the *magnitude* of the component of the *total* magnetic field that is perpendicular to the line of sight and is situated on the plane of the sky. In the derivation of Eq. (6), the $\hat{y}$ axis is chosen to be parallel to the component of the magnetic field on the plane of the sky. Stokes U is defined to be situated on the x-y plane and makes an angle of $\pi/4$ with respect to the $\hat{y}$. The specification of the coordinate system is important because Stokes Q and U are coordinate dependent quantities. Stokes V and I are however, invariants. This implies if the orientation of the magnetic field on the plane of the sky changes (without a change in the line of sight component of the magnetic field), then the observer's measure of Stokes Q and U changes in the context of Eq. (6). This does not change the measure of V. Please see more on this discussion after we have introduced the parameter α in the next section.

Another important factor in this context is FR of the EM wave. FR induces transfer between the Stokes Q and U components. This happens to due to the rotation of the incoming polarization of the EM field due to the line of sight magnetic field component. As the plasma becomes more relativistic, the FR effects in the plasma decreases [43]. In this paper, we have considered a relativistic plasma and hence considered the FR effects on the EM wave to be insignificant. A more realistic calculation must involve a full address of the problem involving both the FR and FC mechanisms.

III. FARADAY CONVERSION FROM POP III STARS

Within the ΛCDM framework of structure formations, dark matter halos begin to be formed around redshifts of $z \sim$ 20-30. Inside of the dark matter halos, Pop III stars were born. Although the final mass of the Pop III stars is determined by several dynamical feed back processes related the pre-stellar gas, typically it is estimated to span between 60-300$M_\odot$.

In this paper, we investigate the CP signals generated when CMB photons pass through the SN remnants of the Pop III stars. A SN generated due to a Pop III star explosion produces a large outburst of energy [37] and a shock wave. As the shock wave propagates through the ambient medium of the explosion, a strong magnetic field and a large number of relativistic electrons are produced. Consequently, CMB photons passing through SN remnants of Pop III stars could be significantly affected by the FC.

Adopting a simple analytic model of the explosion of a Pop III star, first, we estimate the FC induced by one SN remnant of Pop III stars. In order to estimate the angular power spectra of the CP, C_l^{VV}, obtained in the previous section, we need to calculate the FC power spectrum, P_α. Based on the halo model, we evaluate P_α due to SN remnants of Pop III stars.

A. Faraday Conversion due to a Pop III star explosion

Faraday conversion rate α in Eq. (6) is given by [10]

$$\begin{aligned} \alpha(z,\vec{x},\hat{n},\hat{b}) &= \alpha_0 \sin(\theta_B)^{\frac{\gamma+2}{2}}, \\ \alpha_0 &= C_\gamma \frac{e^2}{m_e c} n_{\rm rel} \epsilon_{\rm min} (B_{\rm mag})^{\frac{\gamma+2}{2}} \nu^{-\frac{\gamma+4}{2}}, \end{aligned} \tag{12}$$

where θ_B is the angle between the direction of the line of sight $\hat{n}$ and the magnetic field direction $\hat{b}$, $n_{\rm rel}$ is the number density of relativistic electrons and γ denotes the power-law distribution of the relativistic electrons which described in terms of the Lorentz factor ϵ as $n_{\rm rel}(\epsilon) = n_0 \epsilon^{-\gamma}$ between $\epsilon_{\rm min} < \epsilon < \epsilon_{\rm max}$. The parameter C_γ in Eq. (12) is provided by [10],

$$C_\gamma = \begin{cases} -2\frac{\gamma-1}{\gamma-2}\left(\frac{e}{2\pi m_e c}\right)^{\frac{\gamma+2}{2}}\left[(\nu(z)/\nu_{\rm L})^{\frac{\gamma-2}{2}} - 1\right], & \gamma \neq 2 \\ \left(\frac{e}{2\pi m_e c}\right)^2 \log(\nu(z)/\nu_{\rm L}), & \gamma = 2, \end{cases} \tag{13}$$

where $\nu_{\rm L}$ is the characteristic frequency of the synchrotron emission by electrons at the lower bound $\epsilon_{\rm min}$, which is represented as $\nu_{\rm L} = eB/(2\pi\epsilon_{\rm min} m_{\rm e})$. We picked $\epsilon_{\rm min} = 100$.

When a SN occurs, large amount of energy is injected into the surrounding gas. As a result, the shock is created and, then, relativistic electrons and magnetic fields are generated inside the shocked gas (SN remnants). In order to estimate the FC rate in SN remnants, we evaluate the number density of relativistic electrons $n_{\rm rel}$ and magnetic fields $B_{\rm mag}$, assuming the regime at which the shock front expands adiabatically. This regime is known as the blast wave regime and the dynamics of this regime is expressed in the Sedov similar solution which describes a point blast spherical explosion in an ambient medium [44]. In this solution, the radius of the shock r_s is given by

$$r_s \sim 2 \text{ pc} \left(\frac{E_{\rm SN}}{10^{53}\text{erg}}\right)^{1/5} \left(\frac{\Omega_b h^2}{0.0245}\right)^{-1/5} \left(\frac{1+z}{20}\right)^{-3/5} \left(\frac{t_{\rm age}}{10^6 \text{ yr}}\right)^{2/5}, \tag{14}$$

where $E_{\rm SN}$ is the energy of the SN explosion and $t_{\rm age}$ is the time since the explosion. In Eq. (14), we assume that the shock expands into an ambient medium with the mean baryon mass density $\bar{\rho}_b = \bar{\rho}_{b0}(1+z)^3$ where ρ_{b0} is the mean baryon mass density at the present, although we will discuss the baryon density in more detail below.

The energy $E_{\rm SN}$ generally depends on a mass of the exploded Pop III star. Since Pop III stars are predicted to be massive, 60-300 $M_\odot$, we assume that Pop III stars have 100 $M_\odot$ mass and explode as pair-instability SNe which are 100 times more powerful than typical type II SNe. Therefore, we adopt $E_{\rm SN} = 10^{53}$ ergs in this paper.

The shock wave expands in the interior of a dark matter halo at first. Then the shock wave spreads out to the outside of the halo, because r_s could become larger than the size of the halo as $t_{\rm age}$ increases. We simply assume that the shock continues to expand following Eq. (14) in both the inside and the outside of the halo. Therefore, we set ρ_b to

$$\rho_b = \begin{cases} \rho_b^{\rm halo}, & r_s \leq R_{\rm vir} \\ \bar{\rho}_b, & r_s > R_{\rm vir}, \end{cases} \tag{15}$$

where $R_{\rm vir}$ is the virial radius of the halo and $\bar{\rho}_b$ is the mean baryon mass density in the universe. To obtain the baryon mass density inside of a dark matter halo $\rho_b^{\rm halo}$, we assume that the baryon mass distributes homogeneously inside the virial radius. Accordingly, the baryon mass density in the halo is given by

$$\rho_b^{\rm halo} = \frac{\Omega_b}{\Omega_b + \Omega_c} \frac{3M}{4\pi R_{\rm vir}^3}. \tag{16}$$

The blast wave phase continues until the cooling of the SN remnant becomes effective. One of the important cooling mechanisms is the inverse Compton (IC) scattering. The cooling time, $t_{\rm IC}$, for the IC scattering is independent of temperature and density of the gas,

$$t_{\rm IC} = \frac{3 m_e c}{4\sigma_T \rho_{\rm CMB}} \approx 1.4 \times 10^7 \text{ yr} \left(\frac{1+z}{20}\right)^{-4}, \tag{17}$$

where σ_T is the Thomson cross-section of an electron and $\rho_{\rm CMB}$ is the CMB energy density. Eq. (17) sets an upper limit on $t_{\rm age} \lesssim 10^7$ yr, used for the estimation of r_s in Eq. (14).

Let us evaluate the number density of relativistic electrons. Suppose that the fraction $f_{\rm rel}$ of the explosion energy $E_{\rm SN}$ gets converted into relativistic energy of electrons. For a hydrodynamic shock, the inner radius of the shocked regime (SN remnant) is estimated to be [45]

$$r_p = r_s \left(\frac{\eta}{\eta - 1}\right)^{-1/3} \tag{18}$$

This equation is based on the conservation of mass in the shock enclosed regime, where the density rises by a factor of η. For the case of monoatomic gas, which we adopt here, $\eta = 4$. Therefore, the width of a remnant is $r_s - r_p \sim 0.1 r_s$.

We simply assume that the relativistic electrons are confined in the region between the radius r_p and r_s, whose volume is $V_{\rm rem} = 4\pi(r_s^3 - r_p^3)/3$. Assuming the power-law distribution of the relativistic electrons as mentioned above, we can obtain the normalization n_0 of the distribution from

$$f_{\rm rel} E_{\rm SN} = V_{\rm rem} \int_{\epsilon_{\rm min}}^{\epsilon_{\rm max}} n_0 m_e c^2 \epsilon^{1-\gamma}. \tag{19}$$

In our calculation, we use $\gamma = 2$, $\epsilon_{\rm min} = 100$ and $\epsilon_{\rm max} = 300$.

For magnetic fields, we also introduce the parameter $f_{\rm mag}$ which denotes the fraction of the energy of a Pop III star explosion into magnetic field energy. The magnetic field amplitude $B_{\rm mag}$ is obtained by solving the equation

$$\frac{B_{\rm mag}^2}{8\pi} V_{\rm rem} = f_{\rm mag} E_{\rm SN}. \tag{20}$$

Therefore, the magnetic field amplitude in a Pop III remnant can be approximately given by the following.

$$B_{\rm mag} \sim 70 \ {\rm mG} \left(\frac{t_{\rm age}}{10^6 {\rm yr}}\right)^{-3/5} \left(\frac{E_{\rm SN}}{10^{53} {\rm ergs}}\right)^{1/5} \left(\frac{1+z}{20}\right)^{9/10} \left(\frac{f_{\rm mag}}{0.1}\right)^{1/2}. \tag{21}$$

Although the parameters $f_{\rm rel}$ and $f_{\rm mag}$ are theoretically uncertain, we have set $f_{\rm rel} = 0.1$ and $f_{\rm mag} = 0.1$ in this paper.In these parameters, the typical value of α_0 is given by the following.

$$\alpha_0 \sim 20 \ {\rm pc}^{-1} \left(\frac{t_{\rm age}}{10^6 {\rm yr}}\right)^{-12/5} \left(\frac{E_{\rm SN}}{10^{53} {\rm ergs}}\right)^{4/5} \left(\frac{1+z}{20}\right)^{3/5} \left(\frac{f_{\rm mag}}{0.1}\right) \left(\frac{f_{\rm rel}}{0.1}\right) \left(\frac{\nu}{1{\rm GHz}}\right)^{-3}. \tag{22}$$

In this paper, we take the assumption about the directions of magnetic fields, $\sin(\theta_{\rm B}) \sim 1$, in all SN remnants for simplicity. This implies that we have ignored the line of sight magnetic field and consequently the FR effects associated to it. This assumption is consistent in our case since the FR effects in a relativistic plasma decreases as the plasma becomes more relativistic [43]. However, in a *non-relativistic* plasma, the FR effect is not negligible in order to evaluate the resultant circular polarization via the FC and it is necessary to solve a full set of the polarization transfer equation including the FR and FC simultaneously.

B. Power spectrum of the FC induced by Pop III stars

In the ΛCDM model, Pop III stars are predicted to have formed inside dark matter halos. Therefore, in order to calculate P_α, we can evaluate P_α, based on the halo model [41]. For simplicity, we assume that Pop III stars form in halos with the virial temperature $T_{\rm vir} > 10^4$ K where atomic hydrogen cooling is effective for the collapse. We also assume that *one* Pop III star is formed per halo and consequently, one halo hosts one Pop III SN remnant. Accordingly, we can write the power spectrum for the FC from Pop III star SN remnants in the following way,

$$P_\alpha(z,k) = P_{\rm mat}(z,k) \left| \int_{M_{\rm thr}} dM \ \frac{dn}{dM} b(M,z) \tilde{\alpha}_0(z,k) \right|^2, \tag{23}$$

where $P_{\rm mat}(z,k)$ is the linear matter power spectrum at a redshift z, $b(M,z)$ is the linear bias of a dark matter halos, dn/dM is the mass function, and $\tilde{\alpha}_0$ is the Fourier component of α_0 and given by,

$$\tilde{\alpha}_0(z,k) = \int \frac{d^3\vec{r}}{(2\pi)^3} \alpha_0(z) p_h(\vec{r}) \exp(-i\vec{k}\cdot\vec{r}). \tag{24}$$

where $p_h(\vec{r})$ is the profile of one SN remnant. For simplicity, we assume that the FC rate is homogeneous inside the SN remnant and the profile is given by $p_h(\vec{r}) = 1$ for $r_p < |\vec{r}| < r_s$, otherwise $p_h = 0$.

In Eq. (23), we consider only the halo-halo correlation term of the halo model, and we neglect the one-halo Poisson term. In other words, we take into the correlation between SN remnants in different halos, while we ignore the correlation within a given SN remnant. In this work, we are interested in the correlation of the CP on large scales (the order of 10 Mpc or equivalently $l < 2000$ in terms of multipole). Since the typical size of SN remnants is much smaller, we can neglect the correlation contribution within a given SN remnant. We will discuss in more detail later.

In Eq. (23), $M_{\rm thr}$ is the threshold mass of the halos hosting a Pop III star and corresponds to the virial mass with $T_{\rm vir} = 10^4$ K [46],

$$M_{\rm thr} = 3.5 \times 10^7 h^{-1} \left(\frac{T_{\rm vir}}{10^4 \ {\rm K}}\right)^{3/2} \left(\frac{\Omega_m}{\Omega_m(z)} \frac{\Delta_c}{18\pi^2}\right)^{-2} \left(\frac{1+z}{10}\right)^{-3/2}, \tag{25}$$

where μ is the mean molecular weight and m_p is the proton mass. For a fully ionized plasma, we used, $\mu = 0.6$.

We choose the mass function, dn/dM, to be alternately defined in terms of a multiplicity function $f(\nu)$ as,

$$\frac{dn}{dM}dM = \frac{\bar{\rho}}{M}f(\nu)d\nu. \tag{26}$$

Here $\bar{\rho}$ is the mean matter density in the universe and ν is defined as $\nu = (\delta_c/\sigma_M)^2$ where δ_c is the threshold overdensity of spherical collapses at redshift z and σ_M is the rms linear density fluctuations obtained with a top-hat filter of mass M at an initial time (see [41] and references therein).

For the function $f(\nu)$, we adopt the function proposed by Sheth and Tormen [47]

$$\nu f(\nu) = A(1+\nu_1^{-p})\left(\frac{\nu_1}{2\pi}\right)^{1/2} e^{-\nu_1/2}, \tag{27}$$

where $\nu_1 = a\nu$ with $a = 0.7$, $p = 0.3$ and A is the normalization constant determined by $\int f(\nu)d\nu = 1$. Following Ref. [41], the linear bias, b_ν, is given in terms of ν by

$$b(\nu) = 1 + \frac{\nu - 1}{\delta_c} + \frac{2p}{\delta_c(1+\nu_1^p)}. \tag{28}$$

In Fig. 1, we plot the power spectrum of α, $P_\alpha(z,k)$. As the redshift decreases, the power spectrum amplitude grows. This is simply due to the growth of the density fluctuations, as a result of which the resultant number density of halos becomes larger at lower redshifts. Fig. 1 also shows that the power spectrum depends on the age of SN remnants $t_{\rm age}$ and the observation frequency ν.

An estimation of the power spectrum for α in Fig. 1 at the peak scale ($k \sim 10^{-2}$Mpc^{-1}) can be verified as follows. For $t_{\rm age}$=10^5 yr and ν=1 GHz, we obtain the value of $\tilde{\alpha}_0 \sim 0.2$ Mpc^2. At $z \sim 20$, the integral of dn/dM over M in Eq. (23) gives ~ 1 Mpc^{-3} [46], and the bias factor is $b(M,z) \sim 1$. Since the amplitude of the matter power spectrum at $k \sim 10^{-2}$ is $P(k) \sim 100$ Mpc^3, we obtain $P_\alpha \sim 10$ Mpc at the peak scale from Eq. (23).

Since we consider only the halo correlation term, as shown in Eq. (23), the spectral shape is same as the one of the linear matter power spectrum. However, in general, the Poisson term is non-negligible on small scales. Taking into account the Poisson term, one can expect that the shape of the power spectrum P_α would deviate from the linear matter power spectrum and be enhanced around $k > 10^5$ Mpc^{-1}, which also corresponds to the typical scale of the SN remnants of Pop III stars.

Since we consider only the halo correlation term, as shown in Eq. (23), the spectral shape is same as the one of the linear matter power spectrum. However, in general, the Poisson term is expected to be non-negligible on small scales. Taking into account the Poisson term, one can expect that the shape of the power spectrum P_α would deviate from the linear matter power spectrum and be enhanced around the scale corresponding to the typical scale of the SN remnants of Pop III stars. The average proper size of the remnants of age, $t_{\rm age}$=10^6 years is ~ 10 pc at $z \sim 20$. This corresponds to an apparent angular size of $\sim 10^{-6}$ in degrees. Therefore, the Poisson term could contribute much on angular power spectrum around multipoles of $l \sim 10^6$. Since such scales are too small to observe the angular power spectrum, we do not address the Poisson term in this paper.

IV. RESULTS FOR THE PREDICTED C_l^{VV} FROM POP III STARS

We numerically calculate the angular power spectrum of the CMB CP due to the SN remnants of Pop III stars, substituting the power spectrum P_α obtained in the previous section to Eq. (11).

Although Eq. (11) involves multiple summations of multipoles, we can reduce the calculation. Due to the property of the Wigner-3j symbols in Eq. (A12), the non-zero contributions come from the terms with $l' + L$ is *odd* in Eq. (11). Therefore, non-vanishing I_{lm} requires $m' \neq 0$ in Eq. (11). Under the assumption that the CMB is statistically isotropic, the angular correlation of multipole components V_{lm} defined in Eq. (4) is independent of m. Therefore the calculation with only $m = 0$ in Eq. (11) is enough to obtain the angular power spectrum. Additionally, in order to reduce computational efforts, we ignore the azimuthal dependence due to m''. In other words we just multiply $(2l''+1)$ instead of evaluating a m'' dependent summation.

In Fig. 2, we present the results of $T_{CMB}^2 C_l^{VV}$ in the units of $(\mu K)^2$. Here we assume that Pop III stars exist in high redshifts between $z = 24$ and 17, and we set $\nu = 1$ GHz, $f_{\rm rel} = 0.1$ and $f_{\rm mag} = 0.1$. Although P_α has a peak at $k \sim 10^{-2}$ corresponding to $l \sim 100$, the angular power spectrum of the CMB CP C_l^{VV} peaks at higher $l \sim 2000$. This is because C_l^{VV} is the convolution between the P_α and the E-mode power spectrum. We also show the dependence on $t_{\rm age}$ in Fig. 2.As the SN remnants expand with $t_{\rm age}$ increase, the number density of relativistic electrons and

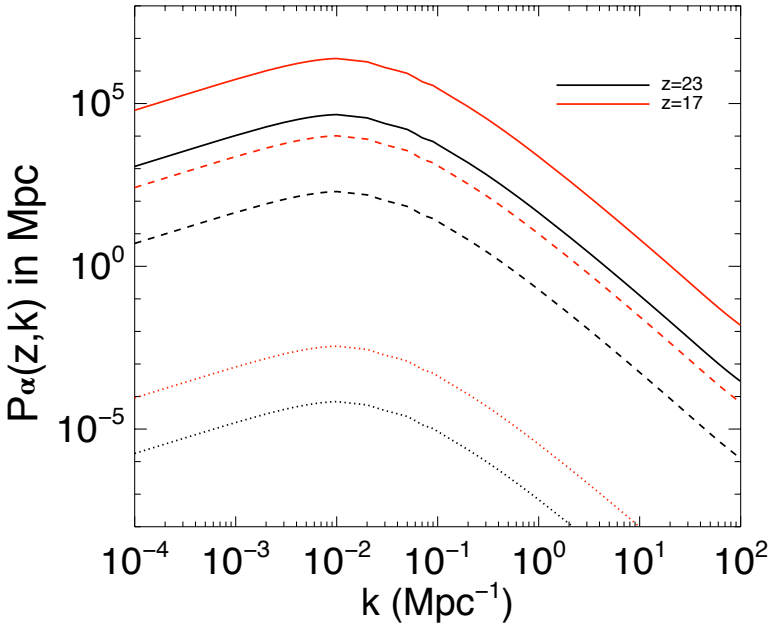

FIG. 1: Power spectra of Faraday conversion generated by the First stars at different redshifts. The unit of $P_\alpha(k,z)$ is in Mpc.The solid lines correspond to $t_{\rm age} = 10^4$ years and $\nu = 1$ GHz. The dashed lines correspond to $t_{\rm age} = 10^5$ years and $\nu = 1$ GHz. Lastly, the dotted lines correspond to $t_{\rm age} = 10^4$ years and $\nu = 30$ GHz. Here, ν is the frequency of the CMB photons observed today.

magnetic field energy decrease. Accordingly the FC becomes ineffective in the case with large $t_{\rm age}$. For comparison, we also plot the angular power spectrum with $\nu = 30$ GHz. The spectrum is strongly sensitive to the frequency of the CMB observation. Although the frequency dependence depends on the power-law index γ of the relativistic electron distributions, the amplitude of C_l^{VV} is proportional to ν^{-6} for the case with $\gamma = 2$.

One can roughly estimate C_l^{VV} in the following way. C_l^{VV} is a convolution between power spectrum of circular polarization coefficient α and that of E-mode polarization and can be approximated to $l^2 C_l^{VV} \sim l^2 C_l^{\alpha\alpha} C_l^{EE}$ where C_l^{EE} and $C_l^{\alpha\alpha}$ are the angular power spectra for CMB E-mode polarization and the FC parameter α, respectively. We are interested in scales $l > 100$. The Limber approximation gives the relation between $C_l^{\alpha\alpha}$ and P_α (given in Fig. 1) as $l^2 C_l^{\alpha\alpha} \sim k P_\alpha(l/r_z)$ where r_z is the radial distance to redshift z and $kr_z \sim l$. For example, at $z \sim 20$, in scales $l \sim 10^3$, $l/r_{z\sim 20}$ corresponds to $k \sim 0.1$ Mpc^{-1}. For $t_{\rm age}$=10^5 yr and ν=1 GHz, including the contributions from all redshifts, at $k \sim 0.1$ Mpc^{-1}, $P_\alpha \sim 10^3$ Mpc from Fig. 1. The angular power spectrum of E-mode polarization is $C_l^{EE} \sim 10^{-2}$ μK^2 at $l \sim 10^3$. Therefore, the resultant angular power spectrum of the CP is $l^2 C_l^{VV} \sim k P_\alpha C_l^{EE} \approx 10^{-2}$ μK^2 for $t_{\rm age} = 10^5$ yr at 1 GHz. This estimation is consistent with our calculated total C_l^{VV} in Fig. 2.

In Fig. 3, we show the redshift dependence of C_l^{VV}. In this case we have only considered remnants with $t_{\rm age}$=10^4 yrs. Fig. 3 conveys that C_l^{VV} decreases with increasing redshift. This is primarily due to the increase in the number density of Pop III stars in lower redshifts directly due to increase in the number of halos. In this paper, although we do not take into account the redshift dependence of the evolution of Pop III star properties, their properties strongly depend on redshift. In particular, the metal pollution due to explosions of Pop III stars make mass of Pop III stars small and, finally, the abundance of Pop III stars are dominated by Pop II stars. These redshift evolutions induce the suppression in the efficiency of the FC in lower redshifts. Therefore, C_l^{VV} in lower redshifts is expected to lower than our estimation. However, this is beyond the scope of this paper.

There are two factors involved in the understanding an order of magnitude estimate for the redshift dependence. One, an increase in the number density of halos with decreasing redshift and two, a given length scale is manifested at a slightly larger angular scale (or at a slightly higher multipole) with decreasing redshift. The dominating effect of increase in the signal due to increase in the number density of halos with decreasing redshift is clearly manifested in Fig. 3. An approximate increase of two orders of magnitude in the power spectrum at a given scale upon decrease of redshift from $z = 23$ to $z = 17$ is shown in Fig. 3. This change is also manifested in Fig. 3 with a similar reduction in the signal between $z = 23$ and $z = 17$.

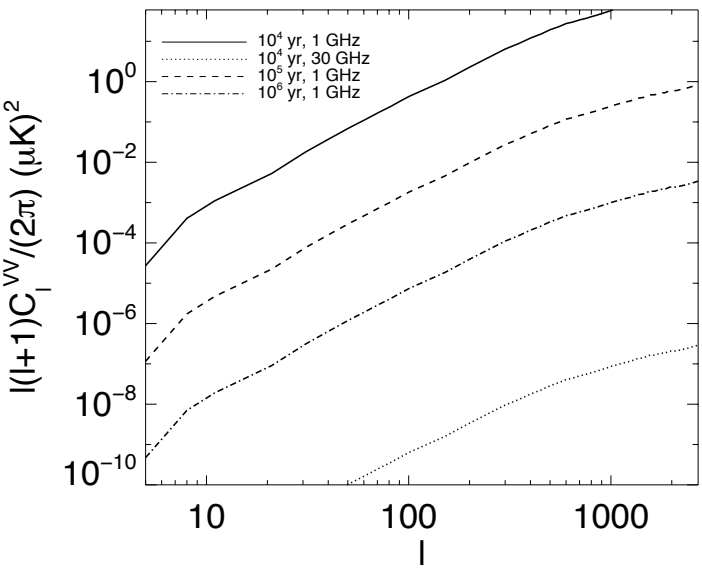

FIG. 2: Angular power spectra of circular polarization from Eq. (11) times $T^2_{\rm CMB}$ in $(\mu{\rm K})^2$. We have chosen a few cases for the age of the remnant of the Pop III explosion, with $10^4 < t_{\rm age} < 10^6$ in years. The frequency of observation of the CMB has been chosen to be $\nu = 1$ and 30 GHz. Other parameters for this plot are described in Sec. IV. In this figure only *one* Pop III star was assumed per halo.

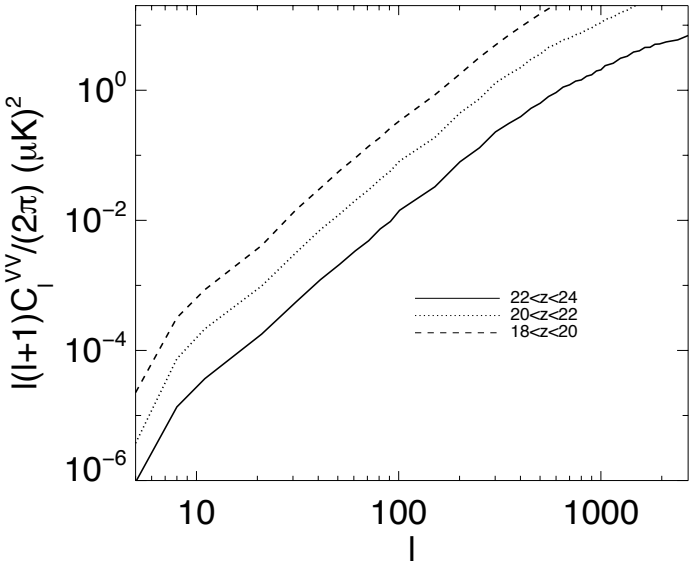

FIG. 3: Angular power spectra of circular polarization from Eq. (11) times $T^2_{\rm CMB}$ in $(\mu{\rm K})^2$. We have chosen a few redshift slices and the age of the remnant of the Pop III explosion to be $t_{\rm age} = 10^4$ in years. The frequency of observation of the CMB has been chosen to be $\nu = 1$ GHz for this plot. Other parameters for this plot are described in Sec. IV.

V. DISCUSSION AND SUMMARY

In this paper, we have studied the CP signals of the CMB, focusing on the Faraday Conversion (FC) caused by the SN remnant of the Pop III star explosions. In the SN remnant, the relativistic electrons are produced and the magnetic fields are amplified. Therefore, during the propagation through the SN remnant, the CMB undergoes FC which transfers some of its linear polarization into circular polarization (CP).

In this paper, we have derived an analytic form for the angular power spectrum of the CMB CP. This analytic form is general to the CP due to the FC. The angular power spectrum is the convolution between the CMB E-mode and the FC rate power spectra.

We have applied this analytic form to estimate the CP of the CMB due to the SN remnants of Pop III stars. Compared with primary E-mode polarization, the amplitude of the produced CP is suppressed by a factor of 10^{-4} in terms of the angular power spectrum for remnants of the Pop III stars with $t_{\rm age} > 10^5$ yr. The efficiency of the FC strongly depends on the frequency of CMB photons. We found that the amplitude of the CP angular power spectrum is proportional to ν^{-6}. The signals of the CP fall off with increasing frequency. As the SN remnant evolution, we adopt the simple analytic model, the Sedov similar solution. In this model, as the SN remnant evolves, the number density of relativistic electrons and the amplification of magnetic fields are suppressed. Therefore, the signals of the CP also decrease with the age of the remnant, $t_{\rm age}$ growing.

Throughout this paper, we have assumed that energy of each Pop III explosion is $E_{\rm SN} = 10^{53}$ ergs. However, $E_{\rm SN}$ depends on various properties of Pop III stars and is theoretically uncertain. However, the produced CP also depends on the energy of the explosion. The angular power spectrum C_l^{VV} is roughly proportional to $E_{\rm SN}^{(16+2\gamma)/10}$ with the spectral index γ of the relativistic electron distribution. For $\gamma = 2$, we retrieve an approximate quadratic dependence of C_l^{VV} on $E_{\rm SN}$. Therefore, the detailed energy distribution of Pop III SNe is required to predict C_l^{VV} precisely. Additionally, there exists the theoretical uncertainty on the conversion of the SN energy into the energies of relativistic electrons and magnetic fields, which we parameterize as $f_{\rm rel}$ and $f_{\rm mag}$. We will address the modeling of these parameters based on simulations in a future work.

We have assumed the direction of the magnetic field generated by their explosions, to be aligned to the $\hat{z}$ axis. In other words, we have assumed $B_{\rm mag} = B_z$. If we relax this assumption, and consider a general direction of $B_{\rm mag}$, we may use $B_z = B_{\rm mag}/\sqrt{3}$ according to the equipartition over the all directions. The signal of CP due to only B_z is then suppressed by a factor of 1/9. In this case, there are additional contribution due B_x and B_y, the components of magnetic field in the $\hat{x}$ and $\hat{y}$ directions. These contributions could be additive or subtractive and a precise estimate is difficult without a more detailed numerical modeling.

In our evaluation of the CMB CP, we ignore the Faraday rotation (FR) effect. The FR arises when the CMB photons pass through a magnetised plasma. Therefore, when the FC of the CMB occurs, the FR is also expected to be effective. Since the FR rotates the direction of the linear polarization, the relative angle between the linear polarization and the magnetic fields changes. Even more, when the FR is efficient, it might be change the sign of the CP due to the FC. Therefore the magnitude and sign of the final CP might depend on the details of the FR in the system. Although the FR due to magnetic fields in intergalactic medium, galaxy clusters and the Milky way has been studied (e.g. [51–53]), the FR of the CMB in SN remnants of Pop III stars has not been addressed yet. In order to evaluate the effect of SN remnants on the CMB linear and circular polarization, it is required to study the FR and FC consistently. We propose to investigate this detail in the future.

In Ref. [12], the signals of the CMB CP due to the propagation through galaxy clusters are predicted that the peak amplitude is 10^{-1} $(\mu{\rm K})^2$ at $l = 10^3$ for $\nu = 1$GHz. Our predicted signals due to the Pop III stars with $t_{\rm age} = 10^4$ yr can dominate these signals. Although the signals due to the Pop III stars with $t_{\rm age} = 10^5$ yr are comparable with these signals around $l \lesssim 10^3$, these can dominate the signals from galaxy clusters on the smaller scales. Even with $t_{\rm age} = 10^6$ yr, the signals from the Pop III SNe would dominate the ones from galaxy clusters at $l > 5 \times 10^3$. Therefore, the Pop III SNe can contribute the CMB CP significantly, in particular, on small scales $l > 10^3$.

We propose that if the future CMB experiments are equipped with CP measuring instruments, the CMB observation can also be used as a probe of the Pop III stars. In addition to the $\langle VV \rangle$ correlations, $\langle TV \rangle$ and $\langle EV \rangle$ correlations are expected to be higher, leading up to a better detection prospect. An unique frequency signature of the CP signal due to the FC and absence of any significant foreground makes CP signal to be a promising probe of the Pop III stars, which are yet unobserved.

Acknowledgments

We thank Eiichiro Komatsu for helpful comments and Tanmay Vachaspati for important discussions. We thank Frank Timmes for helping us with the computing resources for our calculations. We are also grateful for computing

resources at the ASU Advanced Computing Center (A2C2). We convey sepcial thanks to Philip Lubin and Torsten Ensslin for their helpful comments on the understanding of the physics of the Faraday conversion mechanism. SD is supported by a NASA Astrophysics theory grant NNX11AD31G and HT is supported by DOE at the Arizona State University.

[1] M. J. Rees, APJL **153** L1 (1968)
[2] N. Kaiser, MNRAS **202** 1169 (1983)
[3] A. Kosowsky, Annals Phys. **246**, 49 (1996) [astro-ph/9501045].
[4] M. Zaldarriaga and U. Seljak, Phys. Rev. D **55**, 1830 (1997) [astro-ph/9609170].
[5] M. Kamionkowski, A. Kosowsky and A. Stebbins, Phys. Rev. D **55**, 7368 (1997) [astro-ph/9611125].
[6] W. Hu and M. J. White, New Astron. **2**, 323 (1997) [astro-ph/9706147].
[7] J. Kovac, E. M. Leitch, CPryke, J. E. Carlstrom, N. W. Halverson and W. L. Holzapfel, Nature **420**, 772 (2002) [astro-ph/0209478].
[8] G. Hinshaw *et al.* [WMAP Collaboration], Astrophys. J. Suppl. **208**, 19 (2013) [arXiv:1212.5226 [astro-ph.CO]].
[9] S. Weinberg, Cosmology, by Steven Weinberg. ISBN 978-0-19-852682-7.Published by Oxford University Press, Oxford, UK, 2008. (Oxford University Press, 2008)
[10] V. N. Sazonov, Sov. Phys. JETP 29, 578 (1969) [Zh. Eksp. Teor. Fiz. 56, 1065 (1969)].
[11] T. W. Jones, and S. L. Odell, Astrophys. J. , **214**, 522 (1977).
[12] A. Cooray, A. Melchiorri and J. Silk, Phys. Lett. B **554**, 1 (2003) [astro-ph/0205214].
[13] R. Mohammadi, arXiv:1312.2199 [astro-ph.CO].
[14] M. Giovannini, Phys. Rev. D **80**, 123013 (2009) [arXiv:0909.3629 [astro-ph.CO]].
[15] M. Giovannini, Phys. Rev. D **81**, 123003 (2010) [arXiv:1001.4172 [astro-ph.CO]].
[16] R. F. Sawyer, arXiv:1205.4969 [astro-ph.CO].
[17] S. Alexander, J. Ochoa and A. Kosowsky, Phys. Rev. D **79** (2009) 063524 [arXiv:0810.2355 [astro-ph]].
[18] M. Zarei, E. Bavarsad, M. Haghighat, I. Motie, R. Mohammadi and Z. Rezaei, Phys. Rev. D **81**, 084035 (2010) [arXiv:0912.2993 [hep-th]].
[19] I. Motie and S. -S. Xue, Europhys. Lett. **100**, 17006 (2012) [arXiv:1104.3555 [hep-ph]].
[20] R. Mainini, D. Minelli, M. Gervasi, G. Boella, G. Sironi, A. Ba, S. Banfi and A. Passerini *et al.*, JCAP **1308**, 033 (2013) [arXiv:1307.6090 [astro-ph.CO]].
[21] V. Bromm, N. Yoshida, L. Hernquist and C. F. McKee, Nature **459**, 49 (2009) [arXiv:0905.0929 [astro-ph.CO]].
[22] D. J. Whalen, arXiv:1209.4688 [astro-ph.CO].
[23] V. Bromm, P. S. Coppi and R. B. Larson, Astrophys. J. **527**, L5 (1999) [astro-ph/9910224].
[24] T. Abel, G. L. Bryan and M. L. Norman, Astron. Astrophys. **540**, 39 (2000) [astro-ph/0002135].
[25] T. Abel, G. L. Bryan and M. L. Norman, Science **295**, 93 (2002) [astro-ph/0112088].
[26] V. Bromm, P. S. Coppi and R. B. Larson, Astrophys. J. **564**, 23 (2002) [astro-ph/0102503].
[27] F. Nakamura and M. Umemura, Astrophys. J. **548**, 19 (2001) [astro-ph/0010464].
[28] N. Yoshida, K. Omukai and L. Hernquist, arXiv:0807.4928 [astro-ph].
[29] A. Heger and S. E. Woosley, Astrophys. J. **567**, 532 (2002) [astro-ph/0107037].
[30] E. Scannapieco, P. Madau, S. Woosley, A. Heger and A. Ferrara, Astrophys. J. **633**, 1031 (2005) [astro-ph/0507182].
[31] A. Mesinger, B. Johnson and Z. Haiman, [astro-ph/0505110].
[32] D. Kasen, S. E. Woosley and A. Heger, Astrophys. J. **734**, 102 (2011) [arXiv:1101.3336 [astro-ph.HE]].
[33] T. Pan, D. Kasen and A. Loeb, Mon. Not. Roy. Astron. Soc. **422**, 2701 (2012) [arXiv:1112.2710 [astro-ph.HE]].
[34] J. Hummel, A. Pawlik, M. Milosavljevic and V. Bromm, Astrophys. J. **755**, 72 (2012) [arXiv:1112.5207 [astro-ph.CO]].
[35] M. Tanaka, T. J. Moriya, N. Yoshida and K. 'i. Nomoto, Mon. Not. Roy. Astron. Soc. **422**, 2675 (2012) [arXiv:1202.3610 [astro-ph.CO]].
[36] D. J. Whalen, C. L. Fryer, D. E. Holz, A. Heger, S. E. Woosley, M. Stiavelli, W. Even and L. L. Frey, Astrophys. J. **762**, L6 (2013) [arXiv:1209.3457 [astro-ph.CO]].
[37] D. J. Whalen, W. Even, L. H. Frey, J. Smidt, J. L. Johnson, C. C. Lovekin, C. L. Fryer and M. Stiavelli *et al.*, Astrophys. J. **777**, 110 (2013) [arXiv:1211.4979 [astro-ph.CO]].
[38] R. S. de Souza, E. E. O. Ishida, J. L. Johnson, D. J. Whalen and A. Mesinger, arXiv:1306.4984 [astro-ph.CO].
[39] A. Meiksin and D. J. Whalen, arXiv:1209.1915 [astro-ph.CO].
[40] S. P. Oh, A. Cooray and M. Kamionkowski, Mon. Not. Roy. Astron. Soc. **342**, L20 (2003) [astro-ph/0303007].
[41] U. Seljak, Mon. Not. Roy. Astron. Soc. **318**, 203 (2000) [astro-ph/0001493].
[42] A. Kosowsky, [astro-ph/9904102]
[43] T. Beckert, Astrophysics and Space Sciences **288**, 123 (2003)
[44] Sedov, L. I. 1959, Similarity and Dimensional Methods in Mechanics, New York: Academic Press, 1959.
[45] Osterbrock, D. E., & Ferland, G. J. 2006, Astrophysics of gaseous nebulae and active galactic nuclei, 2nd. ed. by D.E. Osterbrock and G.J. Ferland. Sausalito, CA: University Science Books, 2006
[46] R. Barkana and A. Loeb, Phys. Rept. **349**, 125 (2001) [astro-ph/0010468].
[47] R. K. Sheth and G. Tormen, Mon. Not. Roy. Astron. Soc. **308**, 119 (1999) [astro-ph/9901122].

[48] A. Kosowsky, T. Kahniashvili, G. Lavrelashvili, and B. Ratra, Phys. Rev. D **71**, 043006 (2005), [astro-ph/0409767].
[49] D. W. L. Sprung, W. van Dijk, J. Martorell, and D. B. Criger, American Journal of Physics **77**, 552 (2009).
[50] Xu, H., Wise, J. H., & Norman, M. L. 2013, Astrophys. J. , 773, 83
[51] A. Kosowsky and A. Loeb, Astrophys. J. **469**, 1 (1996) [astro-ph/9601055].
[52] H. Tashiro, N. Aghanim and M. Langer, Mon. Not. Roy. Astron. Soc. **384**, 733 (2008) [arXiv:0705.2861 [astro-ph]].
[53] S. De, L. Pogosian and T. Vachaspati, Phys. Rev. D **88**, no. 6, 063527 (2013) [arXiv:1305.7225 [astro-ph.CO]].

Appendix A: Derivation of C_l^{VV}

In this appendix, we derive the angular power spectrum of the CP of the CMB, Eq. (11). As shown in Eq. (6), the observed Stokes parameter V due to the FC is given by

$$V(\hat{n}) = -2\int_{r_*}^{0} dr\; U(r,\vec{x},\hat{n})\alpha(r,\vec{x},\hat{n},\hat{b}). \tag{A1}$$

According to Eq. (12), α is proportional to $(\sin\theta_B)^{(\gamma+2)/2}$ where θ_B is the angle between the line-of-sight direction $\hat{n}$ and the direction of magnetic fields $\hat{b}$. In order to express the θ_B-dependence explicitly, we rewrite α as

$$\alpha(r,\vec{x},\hat{n},\hat{b}) = \alpha_0(r,\vec{x})(\sin\theta_B)^{(\gamma+2)/2}. \tag{A2}$$

For simplicity, we consider only z-direction component of magnetic fields with adopting $\gamma = 2$. In this case, the θ_B-dependence can be written as

$$(\sin\theta_B)^{(\gamma+2)/2} = \sin^2\theta = \frac{1}{2}\sqrt{\frac{32\pi}{15}}\left({}_2Y_2^0(\hat{n}) + {}_{-2}Y_2^0(\hat{n})\right), \tag{A3}$$

where θ is a polar angle component of $\hat{n}$ in a spherical coordinate system $\hat{n} = (\theta,\phi)$ for the sky. We perform the Fourier decomposition of $\alpha_0(r,\vec{x})$,

$$\alpha_0(r,\vec{x}) = \int \frac{d^3k}{(2\pi)^3}\tilde{\alpha}(r,k)\exp(i\vec{k}\cdot\vec{x}). \tag{A4}$$

Accordingly, $\alpha(r,\vec{x},\hat{n},\hat{b})$ is expressed as

$$\alpha(z,\vec{x},\hat{n},\hat{b}) = 2\pi\sqrt{\frac{32\pi}{15}}\int\frac{d^3k}{(2\pi)^3}\tilde{\alpha}(z,k)\left({}_2Y_2^0(\hat{n}) + {}_{-2}Y_2^0(\hat{n})\right)\sum_l(-i)^l j_l(kr)\sum_{m=-l}^{m=l}Y_{lm}^*(\hat{k})Y_{lm}(\hat{n}), \tag{A5}$$

where we use the Rayleigh expansion,

$$e^{i\vec{k}.\vec{x}} = \sum_{lm}4\pi(-i)^l j_l(kr)Y_l^m(\hat{k})Y_l^m(\hat{n}), \tag{A6}$$

with $\hat{k} = \vec{k}/k$.

From Eq. (10), we can write the Stokes parameter U as

$$U(r,\vec{x},\hat{n}) = -\frac{i}{2}\int\frac{d^3k}{(2\pi)^3}\sum_l\sum_{m=-2}^{m=2}E_{lm}\left({}_2G_l^m - {}_{-2}G_l^m\right). \tag{A7}$$

Substituting Eqs. (A5) and (A7) to Eq. (A1) provides

$$\begin{aligned} V(\hat{n}) \;=\; & -8\pi^2 i\sqrt{\frac{32\pi}{15}}\sum_l\sum_{m=-2}^{m=2}\sum_{l'}\sum_{m'=-l'}^{m'=l'}\sum_{l''}\sum_{m''=-l''}^{m''=l''}\int_{r_*}^{0}dr\int\frac{d^3k}{(2\pi)^3}\int\frac{d^3k'}{(2\pi)^3} \\ & \times(-i)^{l+l'+l''}\sqrt{\frac{4\pi}{2l+1}}\tilde{\alpha}(r,k')E_{lm}(k,r)j_{l'}(k'r)j_{l''}(kr)Y_{l'm'}^*(\hat{k}')Y_{l''m''}^*(\hat{k}) \\ & \times\left({}_2Y_l^m(\hat{n}) - {}_{-2}Y_l^m(\hat{n})\right)\left({}_2Y_2^0(\hat{n}) + {}_{-2}Y_2^0(\hat{n})\right)Y_{l'm'}(\hat{n})Y_{l''m''}(\hat{n}). \end{aligned} \tag{A8}$$

Decomposing the Stokes parameter V to spherical harmonics as shown Eq. (4), we obtain

$$\begin{aligned} V_{lm} \;=\; & -8\pi^2 i\sqrt{\frac{32\pi}{15}}\sum_{l'}\sum_{m'=-2}^{m'=2}\sum_{l''}\sum_{m''=-l''}^{m''=l''}\sum_{l'''}\sum_{m'''=-l'''}^{m'''=l'''}\int_{r_*}^{0}dr\int\frac{d^3k}{(2\pi)^3}\int\frac{d^3k'}{(2\pi)^3} \\ & \times(-i)^{l'+l''+l'''}\sqrt{\frac{4\pi}{2l'+1}}\tilde{\alpha}(r,k')E_{l'm'}(k)j_{l''}(k'r)j_{l'''}(kr)Y_{l''m''}^*(\hat{k}')Y_{l'''m'''}^*(\hat{k}) \\ & \times\int d^2\hat{n}\left({}_2Y_{l'}^{m'}(\hat{n}) - {}_{-2}Y_{l'}^{m'}(\hat{n})\right)\left({}_2Y_2^0(\hat{n}) + {}_{-2}Y_2^0(\hat{n})\right)Y_{l''m''}(\hat{n})Y_{l'''m'''}(\hat{n})Y_{lm}(\hat{n}). \end{aligned} \tag{A9}$$

Since the product of two spherical harmonics can be given in terms of $3j$ symbols, the non-zero contributions comes from the terms including ${}_2Y_l^m(\hat{n}){}_{-2}Y_2^0(\hat{n})$ and ${}_{-2}Y_l^m(\hat{n}){}_2Y_2^0(\hat{n})$ which are represented as

$$
\begin{aligned}
{}_2Y_l^m(\hat{n}){}_{-2}Y_2^0(\hat{n}) &= \sum_L \sqrt{\frac{5(2l+1)(2L+1)}{4\pi}} \begin{pmatrix} l & 2 & L \\ m & 0 & m \end{pmatrix} \begin{pmatrix} l & 2 & L \\ 2 & -2 & 0 \end{pmatrix} Y_L^0(\hat{n}), \\
{}_{-2}Y_l^m(\hat{n}){}_2Y_2^0(\hat{n}) &= \sum_L \sqrt{\frac{5(2l+1)(2L+1)}{4\pi}} \begin{pmatrix} l & 2 & L \\ m & 0 & m \end{pmatrix} \begin{pmatrix} l & 2 & L \\ -2 & 2 & 0 \end{pmatrix} Y_L^0(\hat{n}).
\end{aligned} \tag{A10}
$$

Integrating Eq. (A9) over $\hat{n}$ yields

$$
\begin{aligned}
V_{lm} &= -8\pi^2 i \sqrt{\frac{32\pi}{15}} \sum_{l'} \sum_{m'=-2}^{m'=2} \sum_{l''} \sum_{l'''} \sum_{m''+m'''=m} \int_{r_*}^0 dr \int \frac{d^3k}{(2\pi)^3} \int \frac{d^3k'}{(2\pi)^3} \\
&\times (-i)^{l'+l''+l'''} \sqrt{\frac{4\pi}{2l'+1}} \tilde{\alpha}(r,k') E_{l'm'}(r,k) j_{l''}(k'r) j_{l'''}(kr) Y^*_{l''m''}(\hat{k}') Y^*_{l'''m'''}(\hat{k}) I_{lm}.
\end{aligned} \tag{A11}
$$

Here I_{lm} represents the integration over $\hat{n}$,

$$
\begin{aligned}
I_{lm} &= \int d^2\hat{n} \left({}_2Y_{l'}^{m'}(\hat{n}){}_{-2}Y_2^0(\hat{n}) - {}_{-2}Y_{l'}^{m'}(\hat{n}){}_2Y_2^0(\hat{n}) \right) Y_{l''m''}(\hat{n}) Y_{l'''m'''}(\hat{n}) Y_{lm}(\hat{n}) \\
&= \sum_{L,L'} \frac{(2L+1)(2L'+1)}{4\pi} \sqrt{\frac{5(2l+1)(2l'+1)(2l''+1)(2l'''+1)}{4\pi}} \\
&\times \left[\begin{pmatrix} l' & 2 & L \\ 2 & -2 & 0 \end{pmatrix} - \begin{pmatrix} l' & 2 & L \\ -2 & 2 & 0 \end{pmatrix} \right] \begin{pmatrix} l' & 2 & L \\ m' & 0 & -m' \end{pmatrix} \\
&\times \begin{pmatrix} l'' & l''' & L' \\ m'' & -m'' & 0 \end{pmatrix} \begin{pmatrix} L & L' & l \\ -m & 0 & m \end{pmatrix} \begin{pmatrix} l'' & l''' & L' \\ 0 & 0 & 0 \end{pmatrix} \begin{pmatrix} L & L' & l \\ 0 & 0 & 0 \end{pmatrix},
\end{aligned} \tag{A12}
$$

where, for non-zero I_{lm}, $m''+m'''$ should be m. Note that in the above expression, $m'=0$ is not allowed since it requires $l'+L=$even, which is opposed by the first difference term in Eq. (A12) that requires $l'+L$ to be odd in order to have a non-vanishing difference term.

Let us calculate the angular power spectrum of V_{lm}, plugging Eq. (A11) to Eq. (5),

$$
\begin{aligned}
C_l^{VV} &= 64 \frac{32\pi^5}{15} \sum_{l'l''l'''} \sum_{m'=-2}^{m'=2} \sum_{m''+m'''=m} \sum_{L'L''L'''} \sum_{M'=-2}^{M'=2} \sum_{M''+M'''=m} \int dr \int dr' \int \frac{d^3k}{(2\pi)^3} \int \frac{d^3k'}{(2\pi)^3} \int \frac{d^3K}{(2\pi)^3} \int \frac{d^3K'}{(2\pi)^3} \\
&\times \sqrt{\frac{(4\pi)^2}{(2l'+1)(2L'+1)}} \langle \tilde{\alpha}(r,k') \tilde{\alpha}(r',K') \rangle \langle E_{l'm'}(k,r) E_{L'M'}(K,r') \rangle \\
&\times j_{l''}(k'r) j_{l'''}(kr) j_{L''}(K'r') j_{L'''}(Kr') Y^*_{l''m''}(\hat{k}') Y^*_{l'''m'''}(\hat{k}) Y^*_{L''L''}(\hat{K}') Y^*_{L'''L'''}(\hat{K}) I_{lm}(l') I_{lm}(L') \\
&= 64 \frac{32\pi^5}{15} \sum_{l'l''l'''} \sum_{m'=-2}^{m'=2} \sum_{m''+m'''=m} \int dr \int dr' \int \frac{k^2 dk}{(2\pi)^3} \int \frac{k'^2 dk'}{(2\pi)^3} \\
&\times \frac{4\pi}{(2l'+1)} \langle \tilde{\alpha}(r,k') \tilde{\alpha}(r',K') \rangle \langle E_{l'm'}(k,r) E_{L'M'}(K,r') \rangle j_{l''}(k'r) j_{l'''}(kr) j_{l''}(k'r') j_{l'''}(kr') I_{lm}^2.
\end{aligned} \tag{A13}
$$

Since we are interested in the scales corresponding to $l > 100$, we can apply the Limber approximation to Eq. (A13),

$$
\int k^2 dk P(k) j_l(kr) j_l(kr') \approx \frac{\pi \delta(r-r')}{2r^2} P(k)|_{k=l/r}. \tag{A14}
$$

Finally, we obtain the angular power spectrum of the Stokes parameter V as

$$
C_l^{VV} = \frac{128}{15} \sum_{l'l''l'''} \sum_{m'=-2}^{m'=2} \sum_{m''+m'''=m} \int dr \int \frac{k^2 dk}{(2l'+1) r^2} P_\alpha \left(\frac{l''}{r}, r \right) P_{E_{lm}}(k,r) \, j_{l'''}^2(kr) I_{lm}^2, \tag{A15}
$$

where we define the power spectra of α and E_{lm} at a comoving distance r as

$$\langle \alpha(\boldsymbol{k}, r)\alpha^*(\boldsymbol{k}', r)\rangle = (2\pi)^3\delta^3(\boldsymbol{k}-\boldsymbol{k}')P_\alpha(k, r), \quad \langle E_{lm}(\boldsymbol{k}, r)E^*_{lm}(\boldsymbol{k}', r)\rangle = (2\pi)^3\delta^3(\boldsymbol{k}-\boldsymbol{k}')P_E(k, r). \tag{A16}$$

In our final calculation of C_l^{VV}, we have simplified the evaluation of I_{lm} by using Eq. (B2) and Eq. (B4) of Ref. [48] for Wigner-3js with zero azimuthal numbers. For the Wigner-3js with non-zero azimuthal numbers, we have used Eq. (A5c) of Ref. [49] wherever appropriate.